CHEMICAL ENGINEERING TRANSACTIONS
VOL. 113, 2024
A publication of AIDIC
The Italian Association of Chemical Engineering
Online at www.cetjournal.it
Guest Editors: Jeng Shiun Lim, Bohong Wang, Guo Ren Mong, Petar S. Varbanov

ISBN 979-12-81206-14-4; **ISSN** 2283-9216
DOI: 10.3303/CET24113107

Green Synthesis and Characterization of ZnO Nanoparticles using *Annona Muricata* Leaves

Sergio P.R. Avila-Concepción[a], Fanny Samanamud-Moreno[b,*], Héctor Chinchay-Espino[c,d], Gina Zavaleta-Espejo[e], Eiser Valle-Rivera[a], Evelyn Carranza-Segura[f], Segundo Jáuregui-Rosas[b]

[a]Escuela de Física, GMIN-UNT, Universidad Nacional de Trujillo
[b]Departamento de Física, GMIN-UNT, Universidad Nacional de Trujillo
[c]Department of Physics and Astronomy, University of New Hampshire, Durham, NH, 03824, USA
[d]Escuela de Posgrado, GMIN-UNT, Universidad Nacional de Trujillo
[e]Departamento de Ciencias Biológicas, GMIN-UNT, Universidad Nacional de Trujillo
[f]Escuela de Microbiologia, GMIN-UNT, Universidad Nacional de Trujillo
fsamanamud@unitru.edu.pe

Zinc oxide (ZnO) nanoparticles were synthesized by green chemistry from aqueous extracts of *Annona muricata* (Soursop) leaves at different concentrations (25 g/L, 50 g/L, 100 g/L, and 200 g/L), subjected to thermal treatment at 400 °C for 1 h. The obtained nanoparticles were characterized using X-ray diffraction (XRD), UV-Vis spectroscopy, Raman spectroscopy, TEM, photoluminescence (PL) and FTIR techniques. XRD and Raman results confirmed the formation of wurtzite-phase crystallized ZnO nanoparticles with hexagonal structure. Furthermore, the average crystallite size decreased with increasing leaf concentration. The TEM result confirmed the NP size for the concentration of 100 g/L was 8 nm, being consistent with the XRD results. Also, it was determined by PL and UV-Vis that the decrease in crystallite size and band gap was correlated with a lower defect concentration and an increase in particle size. The presence of biological residues in the extract was confirmed by FTIR. It was determined that 100 g/L of *A. muricata* leaf was the optimal concentration to produce ZnO nanoparticles with the smallest crystallite size. In conclusion, it was demonstrated that the developed method is simple and economical, standing out compared to conventional chemical methods due to its environmentally friendly nature and the reduced use of hazardous chemicals; and it has been observed that controlling the amount of *A. muricata* leaves allows for a certain control over the size of the ZnO nanoparticles (NPs).

1. Introduction

Zinc oxide nanoparticles (ZnO NPs) have attracted considerable interest because of their unique physicochemical properties, which make them suitable for a wide range of applications, such as photocatalysis (Lopez et al., 2021), optoelectronics (Shahzad et al., 2021), solar cells (Le et al., 2020), water treatment (Mugumo et al., 2023), among others. However, conventional methods of ZnO NP synthesis often involve the use of hazardous chemicals and high energy consumption, raising concerns about their environmental and health impacts. Therefore, there is growing interest in developing green and sustainable methods for nanoparticle synthesis, commonly referred to as “green synthesis”.

Environmentally friendly methods leverage biological entities, such as plant extracts (Abdelsattar et al., 2024), fungi (Ganesan et al., 2020), and bacteria (Roy et al., 2024), as reducing and stabilizing agents to produce ZnO nanoparticles in a more environmentally benign manner (Soltyz et al., 2021). This approach not only reduces the use of toxic chemicals but also opens up the possibility of fine-tuning the size (Kumar et al., 2013), shape, and properties of nanoparticles by selecting biological sources and specific reaction conditions.

Recent studies have successfully synthesized ZnO nanoparticles using various botanical extracts, revealing that the choice of biological material significantly influences the structural and functional properties of

Paper Received: 7 September 2024; Revised: 24 October 2024; Accepted: 3 November 2024
Please cite this article as: Avila-Concepción S.P., Samanamud Moreno F., Chinchay-Espino H., Zavaleta-Espejo G., Valle-Rivera E., Carranza-Segura E., Jauregui Rosas S., 2024, Green Synthesis and Characterization of ZnO Nanoparticles using Annona Muricata Leaves, Chemical Engineering Transactions, 113, 637-642 DOI:10.3303/CET24113107

nanoparticles. For example, enhanced photocatalytic activity of ZnO nanoparticles synthesized using extracts of *Azadirachta indica*, *Tagetes erecta*, *Chrysanthemum morifolium*, and *Lentinula edodes* has been reported, highlighting the role of phytochemicals in optimizing nanoparticle performance (Lopez et al., 2021). Similarly, precursor materials (Fakhari et al., 2019) and reaction parameters (Ahmed et al., 2017), such as pH (Cervantes et al., 2024) and temperature, have been shown to be crucial in determining the morphology and size of nanoparticles, which in turn affect their potential applications.
However, no references have been found about the effect of the concentration of *A. muricata* leaves, used in the extract for synthesis, on the properties and control of ZnO NPs, for example, the works carried out by (Karthik et al., 2023) and (Morales et al., 2024) where the synthesis is performed for a single concentration of *A. muricata*. Despite the advances, a comprehensive understanding of the synthesis mechanisms and the ability to control the properties of nanoparticles through green synthesis remains limited (Gadewar et al., 2024) or requires equipment such as microwaves and vacuum drying (Selvanathan et al., 2022), among others. This knowledge gap hinders large-scale production and wider application of green-synthesized ZnO nanoparticles. Therefore, the present study aimed to address these challenges by investigating the green synthesis of ZnO nanoparticles using various concentrations of *A. muricata* leaves. This will contribute to the development of more efficient and scalable green synthesis methods, ultimately promoting the adoption of environment-friendly nanotechnological practices.

2. Materials and methods

2.1. Materials

Zinc acetate dihydrate ($Zn(O_2CCH_3)_2(H_2O)_2$) (Merck, 98%) was used, with distilled water as solvent. *Annona muricata* leaves were collected from the garden of the Universidad Nacional de Trujillo, Trujillo, La Libertad, Perú. Taxonomic verification of the leaves was carried out for the Herbarium "*Herbarium Truxillense*" (HUT), registered with code 64409.

2.2. Synthesis of ZnO NP's

The aqueous extract of *A. muricata* leaves was obtained using different leaf masses (2.5, 5, 10 and 20 g), which were washed with distilled water, dried at room temperature, cut into small pieces and immersed in 100 mL of distilled water. Subsequently, the extracts were heated at 90°C for 2h and filtered through a Whatman #2 filter paper.For the synthesis of ZnO nanoparticles, Zinc Acetate dihydrate was added to the extract to obtain 100 mL at 0.2 M, and the mixture was kept under moderate agitation at 70°C for 40 min. Subsequently, the solution was allowed to dry until it formed a gel, which was then subjected to additional drying in an oven at 80°C for 24 h. Finally, the material was washed with distilled water and 96% alcohol followed by annealing at 400°C for 1h in a muffle furnace. This procedure was followed for each extract, at different concentrations.

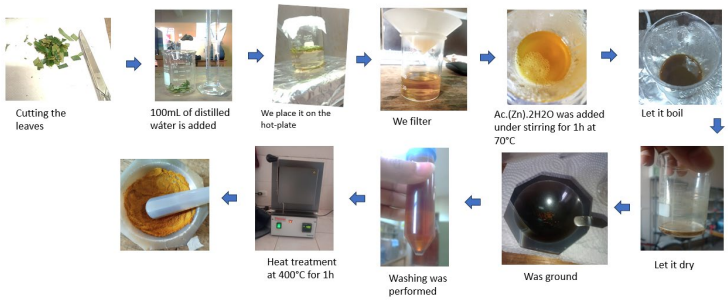

Figure 1: Schematic of the synthesis procedure of ZnO NPs.

2.3. Characterization

The ZnO nanoparticles were characterized by XRD techniques (Rigaku, MiniFlex 600), UV-Vis spectroscopy (PerkinElmer, Lambda 750), Raman spectroscopy (Witec, Alpha 300R), photoluminescence (Perkin Elmer, LS 55), transmission electron microscopy (TEM, Talos F200i) and FTIR spectroscopy (Nicolet iS50, Thermo Scientific).

3. Results and discussion

As shown in Figure 2a, it is observed that all the samples subjected to heat treatment exhibited the formation of Hexagonal wurtzite-phase ZnO. On the other hand, the nanoparticles without thermal treatment, of which the

diffractogram of the sample with no heat treatment (NHT) is shown in representation for the concentration of 100 g/L, did not show uniformity in the formation of ZnO, suggesting that although ZnO was obtained, the structures did not complete their formation because the same number of peaks (crystalline planes) were not obtained for all concentrations, and when applying heat treatment, nanoparticles with a more defined crystalline structure tend to grow more quickly. This behavior is typical in very low-size nanostructures, such as quantum dots or for nanoparticles with surface modification by coating with silent additives, such as the diffractogram presented by (Perhatia et al., 2024). The diffractogram data, presented in Table 1, allowed to analyse the dependence of the average size of the crystallites on the mass of the leaves used in the extract (Figure 2c), making use of the Halder-Wagner method, which considers the broadening of the diffraction peaks as a symmetric Voigt function, offering greater sensitivity to crystallite size distributions, according to the method presented in (Nath, 2020). In general, a decrease in crystallite size was observed with increasing mass, except for the mass of 20 g, where the size increased dramatically.

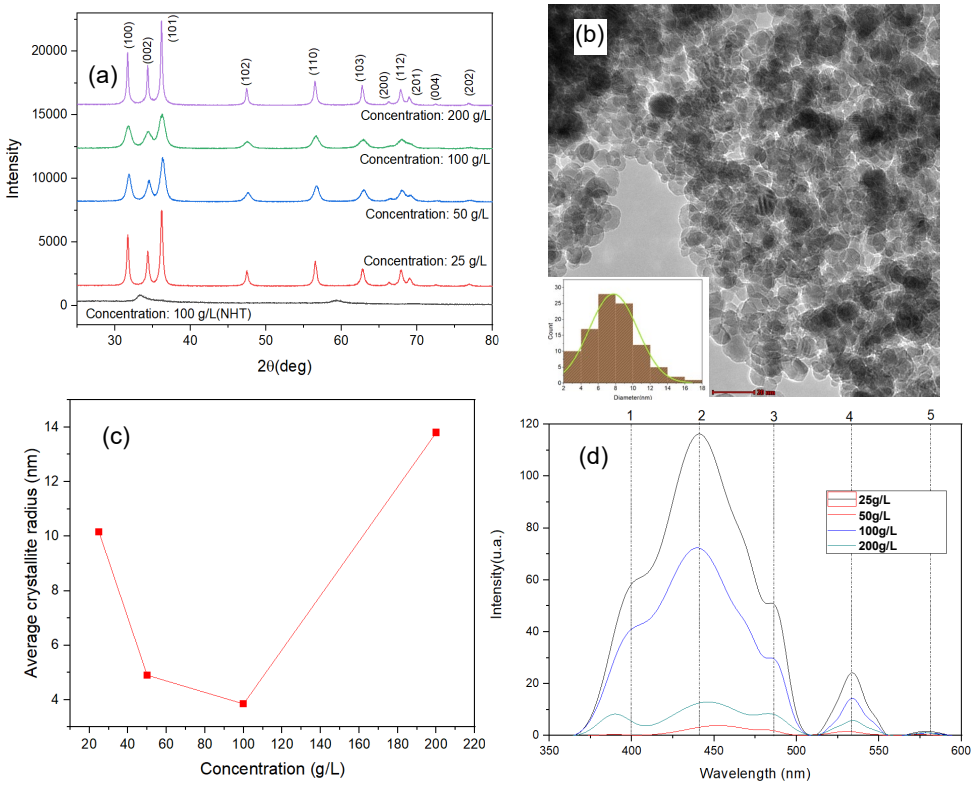

Figure 2: a) X-ray diffractogram for various ZnO NPs concentrations, b) representative TEM image at 100 g/L concentration and size distribution in inset, c) dependence of average crystallite size on leaves concentration, and d) photoluminescence spectra of ZnO NPs.

Table 1: Structural parameters obtained from the XRD patterns.

Concentration(g/L)	D(nm)	a(Å)	c(Å)
25	20.3	3.2533	5.2127
50	9.8	3.2470	5.2040
100	7.7	3.2260	5.2300
200	27.6	3.2557	5.2638

This apparently irregular behavior can be explained because, as mentioned, not all samples after heat treatment resulted in correct crystal formation; however, for those in which ZnO has already been properly formed in Wurzite phase with hexagonal structure, the heat treatment would no longer fulfill the function of crystallization, but rather of particle growth. Furthermore, the formation of ZnO structure prior to heat treatment can be attributed to the variability in the quantity and type of phytoconstituents (Saputra et al., 2024) present in the leaves, as their presence intervenes in the reduction, oxidation, and stabilization of the particle (Shafey, 2020). This variability of the phytoconstituents is evident in the FTIR results; which influences the nucleation and growth

process of the nanoparticles, as described in (Zeghoud et al., 2022). The biomolecules present in the leaves can act as growth agents, facilitating the formation of nuclei and their subsequent growth, leading to a larger final crystallite size. Alternatively, if biomolecules act as stabilizers, preventing further growth of the nuclei, many small nuclei that do not grow significantly can be formed. Thus, up to 100 g/L, there was a preferential reaction to nucleation, increasing the number of nuclei formed, but not growth, following the theory presented in (Thanh et al., 2014), as the solution supersaturation increases, the size of the critical radius of the nuclei decreases.; however, for 20 g, there was a critical point, where greater growth was observed, and the number of nuclei formed decreased.

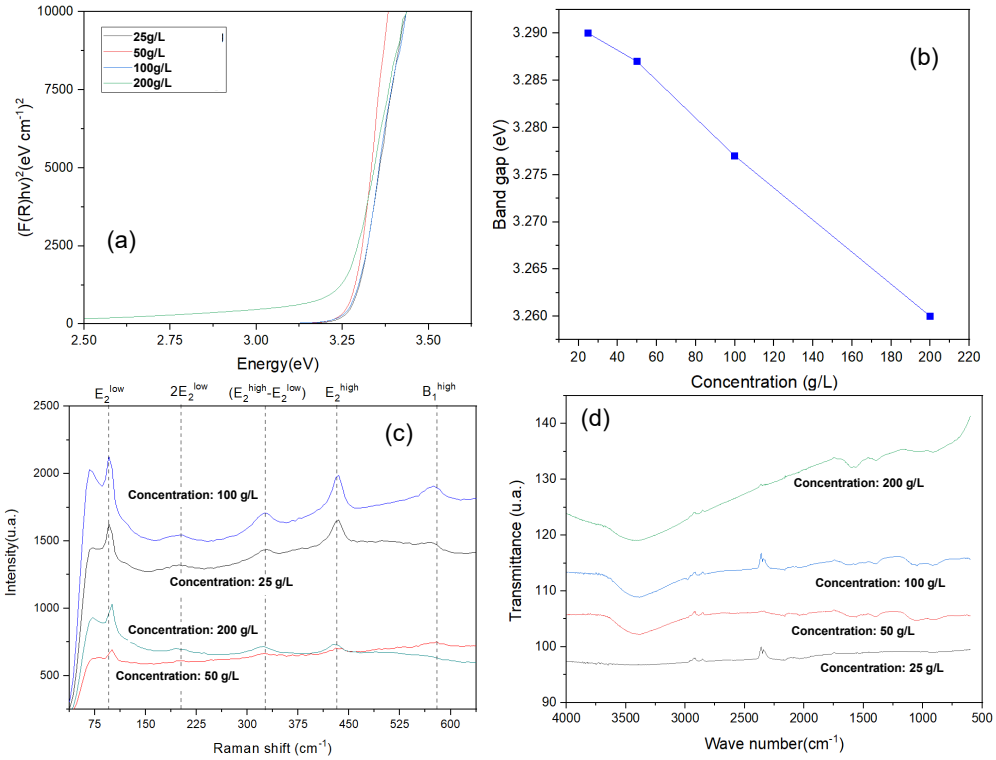

Figure 3: a) UV-Vis reflectance spectra, b) band gap dependence on A. muricata leaves extract concentration, c) Raman spectrum, and d) FTIR spectra of ZnO NPs obtained at various concentrations.

The representative TEM image for the 100 g/L concentration is shown in Figure 2b, with an inset displaying the nanoparticle diameter size distribution histogram. This analysis determined an average nanoparticle size of approximately 8 nm, in agreement with the XRD results for this concentration.

The UV-Vis reflectance spectroscopy spectra, using the Kubelka-Munk function, are presented in figure 3a. Figure 3b shows that the band gap of the nanoparticles tended to decrease as the concentration of the leaves in the extract increased. This result, if explained in terms of quantum confinement, would be contradictory to the XRD findings, where the crystallite size decreases with concentration. However, it is important to note that the relationship between bandgap and particle size does not meet the conditions of quantum confinement, since the bandgap should increase, but we must consider other factors, such as the presence of defects or phytoconstituents, since the relationship between nanoparticle size and bandgap does not consider defect states; therefore, in this case, it was necessary to consider other unusual factors, such as the presence of organic residues and defects in the ZnO nanoparticles, which would increase with the concentration of the mass used in the preparation of the extract, thus increasing the amount of phytoconstituents, which can significantly influence the electronic and optical properties of the samples, introducing energy states within the band, as mentioned in (Van de Walle et al., 2011). This research suggests that increasing the concentration of the constituents, in this case increasing the leaf mass, could lead to increased defect formation, up to a saturation point for a concentration of 200 g/L of leaves. These defects can introduce intermediate states within the band gap, causing its reduction.

In the Raman spectra (Figure 3c), E_2^{low}, E_2^{high} bands are typical Raman active (nonpolar) modes of ZnO, confirming its formation under the experimental conditions; $2E_2^{low}$ is the second-order Raman mode, (E_2^{high} – E_2^{low}) corresponds to the second-order Raman mode from zone boundary phonons, and B_1^{high} is a silent mode,

which were activated due to the presence of defects, the presence of these defects can be confirmed by photoluminescence spectroscopy.

The photoluminescence (PL) spectra are presented in Figure 2d, from which it was identified that band 1, located in the UV region, is close to the absorption edge, and is due to the emission from the band edge, while band 4, located in the visible region, corresponds to the existence of defects, and tends to increase with the decrease in particle size (Nadupalli et al., 2021). The highest intensity was observed at concentrations of 2.5 g, 10 g, 20 g, 5 g from highest to lowest, so that it can be seen how the concentration of defects decreases. Thus, the nanoparticles tended to decrease in defect concentration as the concentration of A. muricata leaves increased, except for the concentration of 5 g, which decreases below the concentration of 20 g. When comparing the results obtained by XRD and UV-Vis spectroscopy, it was observed that as the average crystallite size and band gap decreased, the concentration of defects in the sample decreased. Point defects, such as Zinc and Oxygen vacancies and Zinc and Oxygen interstitials, add new energy levels within the band, thus decreasing the bandgap.

FTIR spectra (Figure 3d) show the presence of biological residues from the *A. muricata* leaves extract used during the synthesis, which did not coincide for all cases, indicating the difference in the presence of phytoconstituents at each concentration. For all bands except the 25 g/L concentration, they presented the bands at 3404.07 cm^{-1} corresponding to the O-H bond and the 1052.33 cm^{-1} band corresponding to the C-OH bond, both corresponding to the alcohol group, in addition to the 1396.32 cm^{-1} band belonging to the CH_3 alkane group; for concentrations of 25, 100 and 200 g/L, they presented the bands at 2349.51cm^{-1} corresponding to carbon residues; for the 25, 50 and 100 g/L samples they presented bands at 2039.73cm^{-1}; and for all leaf mass quantities, the 2898.26 cm^{-1} band corresponding to the CH and CH_2 groups of the alkenes was present. These biocompound residues may contaminate the sample or cause defects in the structure; however, they do not significantly alter the crystalline structure of the material because the network parameters obtained by XRD do not show such alteration.

4. Conclusions

XRD analysis revealed that ZnO nanoparticles obtained from *Annona muricata* extracts were formed in the hexagonal wurtzite phase at all concentrations. The average crystallite size decreased with increasing leaf concentration, except for the 200 g/L concentration, which was attributed to the formation of ZnO prior to thermal treatment caused by the excess of phytoconstituents. The TEM result confirmed the NP size for the concentration of 100 g/L was 8 nm, being consistent with the XRD results. UV-Vis and photoluminescence results indicated that the decrease in crystallite size and band gap was correlated with a lower concentration of defects and an increase in particle size. Finally, FTIR spectroscopy confirmed the presence of biological residues in the extract, different for each leaf mass concentration used in the synthesis, which could introduce defects without significantly altering the crystal structure. Thus, 100 g/L of *A. muricata* leaves was determined to be the optimal concentration to produce nanoparticles with a smaller crystallite size. The developed method has been shown to be simple, economical, and avoids the use of toxic strong bases; it has been observed that controlling the number of *A. muricata* leaves allows the size of the ZnO NPs to be controlled. This research could be improved by quantifying the phytoconstituents in the leaves, which were not analyzed due to the need for more detailed investigation.

Acknowledgments

Grateful acknowledgment is extended to Prociencia del Consejo Nacional de Ciencia, Tecnología e Innovación Tecnológica (CONCYTEC) for financial support under contract N°. PE501083008-2023-PROCIENCIA. Appreciation is also given to the Laboratorio de Análisis Instrumental of the Facultad de Ingeniería Agroindustrial at the Universidad Nacional de Trujillo for supporting the FTIR analysis.

References

Abdelsattar, A. S., Kamel, A. G., Atef Eita, M., Elbermawy, Y., and El-Shibiny, A., 2024, The cytotoxic potency of green synthesis of zinc oxide nanoparticles (ZnO-NPs) using Origanum majorana, Materials Letters, 367(136654), 136654.

Ahmed, S., Annu, Chaudhry, S. A., and Ikram, S., 2017, A review on biogenic synthesis of ZnO nanoparticles using plant extracts and microbes: A prospect towards green chemistry, Journal of Photochemistry and Photobiology. B, Biology, 166, 272–284.

Cervantes-Gaxiola, M. E., Vázquez-González, F. A., Rios-Iribe, E. Y., Méndez-Herrera, P. F., and Leyva, C., 2024, Effect of pH on the green synthesis of ZnO nanoparticles using Sorghum bicolor seed extract and their application in photocatalytic dye degradation, Materials Letters, 372(136982), 136982.

Fakhari, S., Jamzad, M., and Kabiri Fard, H., 2019, Green synthesis of zinc oxide nanoparticles: a comparison, Green Chemistry Letters and Reviews, 12(1), 19–24.

Gadewar, M., Prashanth, G. K., Ravindra Babu, M., Dileep, M. S., Prashanth, P. A., Rao, S., Mahadevaswamy, M., Kumar Ghosh, M., Singh, N., Mandotra, S. K., Chauhan, A., Rustagi, S., Yogi, R., Chinnam, S., Ali, B., Ercisli, S., and Orhan, E., 2024, Unlocking nature's potential: Green synthesis of ZnO nanoparticles and their multifaceted applications – A concise overview, Journal of Saudi Chemical Society, 28(1), 101774.

Ganesan, V., Hariram, M., Vivekanandhan, S., and Muthuramkumar, S., 2020, Periconium sp. (endophytic fungi) extract mediated sol-gel synthesis of ZnO nanoparticles for antimicrobial and antioxidant applications, Materials Science in Semiconductor Processing, 105(104739), 104739.

Karthik, M., Ragunath, C., Krishnasamy, P., Paulraj, D. Q., and Ramasubramanian, V., 2023, Green synthesis of zinc oxide nanoparticles using Annona muricata leaf extract and its antioxidant and antibacterial activity, Inorganic chemistry communications, 157(111422), 111422.

Le T.T.N., Le V.C., Le T.P., Nguyen T.T.M., Ho H.D., Le K.H., Tran M.H., Nguyen T.H., Pham T.L.C., Nam H.M., Phong M.T. and Hieu N.H., 2020, Synthesis of Zinc Oxide/Reduced Graphene Oxide Composites for Fabrication of Anodes in Dye-Sensitized Solar Cells, Chemical Engineering Transactions, 78, 61-66.

López-López, J., Tejeda-Ochoa, A., López-Beltrán, A., Herrera-Ramírez, J., and Méndez-Herrera, P., 2021, Sunlight photocatalytic performance of ZnO nanoparticles synthesized by green chemistry using different botanical extracts and zinc acetate as a precursor, Molecules, 27(1), 6.

Mohan Kumar, K., Mandal, B. K., Kiran Kumar, H. A., and Maddinedi, S. B., 2013, Green synthesis of size controllable gold nanoparticles, Spectrochimica Acta. Part A, Molecular and Biomolecular Spectroscopy, 116, 539–545.

Morales-Ruiz, M.C., Abud-Archila, M., Ventura-Canseco, L. M. C., Gutiérrez-Miceli, F. A., Valdez-Salas, B., and Luján-Hidalgo, M. C., 2024, Biological properties of ZnO phytonanoparticles obtained from Annona muricata L. fruit pulp for possible co-administration with probiotics strains, Journal of microbiology, e9963–e9963.

Mugumo R., Ichipi E.O., Tichapondwa S.M. and Chirwa E.M.N., 2023, Bandgap Tailoring of ZnO Using Metallic Sulphides for Enhanced Visible-light-active Photocatalytic Water Treatment, Chemical Engineering Transactions, 103, 829-834

Nadupalli, S., Repp, S., Weber, S., and Erdem, E., 2021, About defect phenomena in ZnO nanocrystals. Nanoscale, 13(20), 9160–9171.

Nath, D., Singh, F., and Das, R., 2020, X-ray diffraction analysis by Williamson-Hall, Halder-Wagner and size-strain plot methods of CdSe nanoparticles- a comparative study. Materials Chemistry and Physics, 239 (122021), 122021.

Perhaţia, I., Mureşan, L. E., Belcovici, A., Popa, A., Borodi, G., Mesaroş, A., and Barbu Tudoran, L., 2024. Influence of different additives on the morphology, defect state and luminescence of ZnO nanoparticles. Colloids and Surfaces. A, Physicochemical and Engineering Aspects, 684(133102), 133102.

Roy, T., Basak, N., Mainak, S., Das, S., Ali, S. I., and Islam, E., 2024, Burkholderia sp. EIKU21 mediated synthesis of biogenic ZnO nanoparticle–based pigment for development of antibacterial cotton fabric through nanocoating. Biomass Conversion and Biorefinery. 1-16.

Saputra, I. S., Nurfani, E., Fahmi, A. G., Saputro, A. H., Apriandanu, D. O. B., Annas, D., and Yulizar, Y., 2024, Effect of secondary metabolites from several leaf extracts on the green synthesized-ZnO nanoparticles, Vacuum, 227(113434), 113434.

Selvanathan, V., Aminuzzaman, M., Tan, L. X., Win, Y. F., Guan Cheah, E. S., Heng, M. H., Tey, L.-H., Arullappan, S., Algethami, N., Alharthi, S. S., Sultana, S., Shahiduzzaman, M., Abdullah, H., and Aktharuzzaman, M., 2022, Synthesis, characterization, and preliminary in vitro antibacterial evaluation of ZnO nanoparticles derived from soursop (Annona muricata L.) leaf extract as a green reducing agent, Journal of Materials Research and Technology, 20, 2931–2941.

Shafey, A. M. E., 2020, Green synthesis of metal and metal oxide nanoparticles from plant leaf extracts and their applications: A review. Green Processing and Synthesis, 9(1), 304–339.

Shahzad, S., Javed, S., and Usman, M., 2021, A review on synthesis and optoelectronic applications of nanostructured ZnO, Frontiers in Materials, 8.

Soltys, L., Olkhovyy, O., Tatarchuk, T., and Naushad, M., 2021, Green synthesis of metal and metal oxide nanoparticles: Principles of green chemistry and raw materials, Magnetochemistry, 7(11), 145.

Thanh, N. T. K., Maclean, N., and Mahiddine, S., 2014, Mechanisms of nucleation and growth of nanoparticles in solution. Chemical Reviews, 114(15), 7610–7630.

Van de Walle, C. G., and Janotti, A., 2011, Advances in electronic structure methods for defects and impurities in solids, Physica Status Solidi. B, Basic Research, 248(1), 19–27.

Zeghoud, S., Hemmami, H., Ben Seghir, B., Ben Amor, I., Kouadri, I., Rebiai, A., Messaoudi, M., Ahmed, S., Pohl, P., and Simal-Gandara, J., 2022, A review on biogenic green synthesis of ZnO nanoparticles by plant biomass and their applications, Materials Today. Communications, 33(104747), 104747.